Yee Siong Lee received the B.E. and the M.E. degree in Communication and Computer in National Institute of Malaysia, Malaysia in 2009 and 2010 respectively. He is currently pursuing his Ph.D. degree at Deakin University, Australia. His research interests include biomedical applications & signals processing, sensors networks and radar signal processing.

Pubudu N. Pathirana was born in 1970 in Matara, Sri Lanka, and was educated at Royal College Colombo. He received the B.E. degree (first class honors) in electrical engineering and the B.Sc. degree in mathematics in 1996, and the Ph.D. degree in electrical engineering in 2000 from the University of Western Australia, all sponsored by the government of Australia on EMSS and IPRS scholarships, respectively. He was a Postdoctoral Research Fellow at Oxford University, Oxford, a Research Fellow at the School of Electrical Engineering and Telecommunications, University of New South Wales, Sydney, Australia, and a Consultant to the Defence Science and Technology Organization (DSTO), Australia, in 2002. He was a visiting associate professor at Yale University in 2009. Currently, he is an Associate Professor with the School of Engineering, Deakin University, Geelong, Australia and his current research interests include mobile/wireless networks, rehabilitation robotics, and radar array signal processing.

Robin J. Evans received the B.Eng degree in electrical engineering from The University of Melbourne, Melbourne, VIC, Australia, in 1969, and the Ph.D. degree from the University of Newcastle, Callaghan, N.S.W. Australia, in 1975. In 1977 he took up an academic position at the University of Newcastle, where he served as Head of the Department of Electrical and Computer Engineering and Co-Director of the ARC Centre on Industrial Control Systems. In 1992 he moved to the University of Melbourne, where he has served as Head of the Department of Electrical and Electronic Engineering, Research Leader for the Cooperative Centre for Sensor Signal and Information Processing, Director of the Centre for Networked Decision Systems, Dean of Engineering, and Director of NICTA Victoria. He is currently Head of the Department of Electrical and Electronic Engineering and Director of the Defence Science Institute. His research has ranged across many areas including theory and applications in industrial control, radar systems, signal processing and telecommunications. He is a Fellow of the Australian Academy of Science, a Fellow of the Australian Academy of Technological Sciences and Engineering, and Fellow of IEEE.

Christopher L. Steinfort is currently a Respiratory and Sleep Physician with University Hospital Geelong, Geelong, VIC, Australia. He received the M.B.B.S. degree from the University of Melbourne, Melbourne, VIC, in 1978. He is a fellow of the College Physicians, Australia, the Royal Australasian College of Physicians, Australia, and the American College of Chest Physicians. He is also the Director of the Geelong respiratory function and Sleep Medicine Laboratory while he has been a member of numerous societies, including the British, American, Australian, and New Zealand Thoracic Societies.

Separation of Doppler Radar based Respiratory Signatures

Yee Siong Lee · Pubudu N. Pathirana · Robin J. Evans · Christopher L. Steinfort

Abstract Respiration detection using microwave Doppler radar has attracted significant interest primarily due to its unobtrusive form of measurement. With less preparations in comparison to attaching physical sensors on the body or wearing special clothing, Doppler radar for respiration detection and monitoring is particularly useful for long-term monitoring (LTM) applications such as sleep studies (i.e sleep apnea, SIDS). However, motion artefacts and interference from multiple sources limit the widespread use and the scope of potential applications of this technique. Utilizing the recent advances in Independent Component Analysis (ICA) and multiple antenna configuration schemes, this work investigates the feasibility of decomposing respiratory signatures into each subject from the Doppler based measurements. Experimental results demonstrated that fastICA is capable of separating two distinct respiratory signatures from two subjects adjacent to each other even in the presence of apnea. In each test scenario, the separated respiratory patterns correlate closely to the reference respiration strap readings. The effectiveness of fastICA in dealing with the mixed Doppler radar respiration signals confirms its applicability in healthcare applications, especially in long-term home based monitoring as it usually involves at least two people in the same environment (i.e. two people sleeping next to each other). Further, the use of fastICA to separate involuntary movements such as the arm swing from the respiratory signatures of a single subject was explored in a multiple antenna environment. The separated respiratory signal indeed demonstrated a high correlation with the measurements made by a respiratory strap used currently in clinical settings.

Keywords Doppler radar · respiration pattern · Source Separation · fastICA

Yee Siong Lee · Pubudu N Pathirana
School of Engineering, Deakin University, Australia
E-mail: yeel@deakin.edu.au
E-mail: pubudu.pathirana@deakin.edu.au

Robin Evans
Department of Electrical and Electronic Engineering & The Melbourne University, Australia.
E-mail: robinje@unimelb.edu.au

Christopher L. Steinfort
University Hospital Geelong,
Geelong, VIC, Australia
E-mail: chris@steinfortrespiratory.com.au

1 Introduction

Vital sign monitoring using microwave Doppler radar has become an area of special interest for long term respiratory monitoring applications. This form of respiration sensing mechanisms provide numerous additional advantages such as a non-contact form of measurement, robustness and insensitivity to environmental parameters (temperature, lighting etc.). Essentially, in long-term monitoring environments, the characteristic of penetrating through the fabric allows the subjects to wear comfortable clothing and facilitates information capture in a truly natural environment. This is in stark contrast to the currently used chest straps, where, in addition to patient discomfort, the measuring system interferes with the physiological function of respiration due to the physical chest strap causing true breathing information to be inherently corrupted by the measurement system itself.

The use of microwave Doppler radar as a non-contact technique in human vital sign monitoring has been widely reported in a number of research articles (see, for instance [18, 19, 28, 29]). All these demonstrated the fea-

sibility and capability of Doppler radar in capturing human respiration by measuring the change in the frequency of the transmitted signal due to the movement of the abdomen during the process of inhalation and exhalation. Furthermore, Lee *et al.* [16,17] demonstrated that Doppler radar is capable of capturing different respiratory dynamics which include normal breathing, fast breathing, apnea state as well as different rates of inhalation and exhalation accurately when the motion artefacts are appropriately excluded.

Most of the reported results focused on obtaining non-contact respiration measurements for a single subject. In many practical applications, the received signal can easily be adversely affected when there is more than one subject present in the immediate neighbourhood; especially in a home based, long term monitoring application where the subjects share a bed with the partner. Thus, it is necessary to take this case into account for the Doppler radar system to be able to consistently measure the relevant respiratory signatures when subjected to multiple competing signals. In certain earlier work of source separation in Doppler radar signal processing, Alexander *et al.* [26] have demonstrated the use of real analytical constant modulus algorithm (RACMA) to separate certain human body motions and the respiratory signal from the received signals. The results reported in the paper used the wider frequency range of the motion artefacts compared to the targeted normal breathing frequency to clearly identify two distinct sources present when the experiment was conducted under normal breathing conditions.

Furthermore, Olga *et al.* [3] demonstrated the use of single and multiple antenna systems (SIMO/MIMO) in sensing multiple subjects using Doppler radar. Here, the experimental results indicated that it is possible to separate respiratory sources through multiple antenna configuration schemes albeit the experiment considered only the continuous breathing of subjects and the signal analysis was entirely based on the Fast Fourier transform (FFT). This is unlikely in the case for a number of potential applications where abnormal breathing patterns, for instance, apnea symptoms are present and hence FFT analysis is no longer suitable to represent the respiration signal state [16,17]. Therefore, it is also vital to analyse the subject's respiration patterns along with the respiration rate [30]in the presence of possible abnormal breathing patterns.

Initially, in this paper, mixed normal breathing signals from two subjects at different respiratory frequencies were simulated. Then, we demonstrated the capabilities of the fastICA algorithm in separating the simulated baseband respiratory sources and evaluated the performance against the former FFT based approach as

well as the comparison on the distinct signal patterns. In reality, the mixing could be different from the simulation, thus, we first explore the use of multiple Doppler radar modules in acquiring the respiration signals from two subjects and performed the fastICA algorithm on the mixed signal to further evaluate the effectiveness of the separation algorithm. We also extended the analysis to consider a mixture of signals composed of normal and abnormal breathing patterns as listed in section 3. In this paper, for simplicity, we performed the experiments using two subjects for each scenario.

The remainder of this paper is organized as follows: Section 2 provides the theoretical background relevant to Doppler radar in measuring respiratory function including the derivation of the mixed respiration signal model involving multiple subjects. Section 2.2 describes the separation algorithm fastICA implemented with the mixed received Doppler radar signals and Section 3 describes the experimental mechanism employed for data acquisition for multiple respiratory sources as well as for artefact removal. Section 4 discusses the performance of the source separation algorithm on the simulated baseband signals and on the real practical experimentation involving the two different cases of breathing scenarios. Concluding remarks are given in Section 6.

2 Background

2.1 Respiration Sensing Using Doppler Radar

In respiration detection using the microwave Doppler radar, the occurrence of Doppler shift is caused by the movement of the abdomen, $x(t)$ and this effect can be observed from the modulated reflected signal as a phase representation. The phase modulated signal is proportional to the time varying chest displacement. In a homodyne Doppler radar system, a monotonic source of electromagnetic wave is transmitted continuously and can be represented as

$$T(t) = A cos(2\pi f_0 t) + \phi(t), \qquad (1)$$

where A, f_0 are the amplitude and frequency of the transmitted signal respectively. $\phi(t)$ is the arbitrary phase noise of the signal source. In a single subject environment, the phase modulated signal at the receiving end with a nominal distance d_0 caused by the movement of the abdomen during respiration activities can be expressed as

$$R(t) \approx cos(2\pi f_0 t - \frac{4\pi d_0}{\lambda} - \frac{4\pi x(t)}{\lambda} + \phi(t - \frac{2d_0}{c})), \quad (2)$$

In a quadrature receiver, the reflected signal is further expressed as:

$$I(t) = cos(\frac{4\pi d_0}{\lambda} + \frac{4\pi x(t)}{\lambda} + \Delta\phi(t)), \tag{3}$$

$$Q(t) = sin(\frac{4\pi d_0}{\lambda} + \frac{4\pi x(t)}{\lambda} + \Delta\phi(t)). \tag{4}$$

In a multiple subject (N) environment, the modulated signal of each person due to respiration is R_i where $i = 1, 2, ..., N$ referring to each subject and can be expressed as

$$R_1(t) \approx cos(2\pi f_0 t - \frac{4\pi d_0}{\lambda} - \frac{4\pi x_1(t)}{\lambda} + \phi(t - \frac{2d_0}{c}))$$

$$R_2(t) \approx cos(2\pi f_0 t - \frac{4\pi d_0}{\lambda} - \frac{4\pi x_2(t)}{\lambda} + \phi(t - \frac{2d_0}{c}))$$

$$\vdots$$

$$R_N(t) \approx cos(2\pi f_0 t - \frac{4\pi d_0}{\lambda} - \frac{4\pi x_N(t)}{\lambda} + \phi(t - \frac{2d_0}{c}))$$
$$\tag{5}$$

Considering the reflected signal from each target is instantaneously linearly mixed, for instance in the case of $N = M = 2$ where N is the number of subjects and M is the number of transceivers, the received signal (observation) can be represented by

$$\begin{bmatrix} Receiver_1(t) \\ Receiver_2(t) \end{bmatrix} = \begin{bmatrix} a_{11} & a_{12} \\ a_{21} & a_{22} \end{bmatrix} \begin{bmatrix} R_1(t) \\ R_2(t) \end{bmatrix}. \tag{6}$$

where a_{ij} are the mixing parameters. In general, for $N = M = X$, where $X = 2, 3, ...N$, equation 6 can be represented as follows:

$$\begin{bmatrix} Receiver_1(t) \\ Receiver_2(t) \\ \vdots \\ Receiver_M(t) \end{bmatrix} = \begin{bmatrix} a_{11} & a_{12} & \cdots & a_{1N} \\ a_{21} & a_{22} & \cdots & a_{2N} \\ \vdots & \vdots & \cdots & \vdots \\ a_{M1} & a_{M2} & \cdots & a_{MN} \end{bmatrix} \begin{bmatrix} R_1(t) \\ R_2(t) \\ \vdots \\ R_N(t) \end{bmatrix}. \tag{7}$$

In quadrature receiver architecture, generally, equation 3 can be structured as

$$\begin{bmatrix} I_1 \\ I_2 \\ \vdots \\ I_M \end{bmatrix} = \begin{bmatrix} a_{11} & a_{12} & \cdots & a_{1N} \\ a_{21} & a_{22} & \cdots & a_{2N} \\ \vdots & \vdots & \cdots & \vdots \\ a_{M1} & a_{M2} & \cdots & a_{MN} \end{bmatrix} \begin{bmatrix} cos(\theta + Cx_1(t) + \Theta) \\ cos(\theta + Cx_2(t) + \Theta) \\ \vdots \\ cos(\theta + Cx_N(t) + \Theta) \end{bmatrix} \tag{8}$$

while equation 4 is represented as

$$\begin{bmatrix} Q_1 \\ Q_2 \\ \vdots \\ Q_M \end{bmatrix} = \begin{bmatrix} a_{11} & a_{12} & \cdots & a_{1N} \\ a_{21} & a_{22} & \cdots & a_{2N} \\ \vdots & \vdots & \cdots & \vdots \\ a_{M1} & a_{M2} & \cdots & a_{MN} \end{bmatrix} \begin{bmatrix} sin(\theta + Cx_1(t) + \Theta) \\ sin(\theta + Cx_2(t) + \Theta) \\ \vdots \\ sin(\theta + Cx_N(t) + \Theta) \end{bmatrix} \tag{9}$$

where $\theta = \frac{4\pi d_0}{\lambda}$, $C = \frac{4\pi}{\lambda}$ and $\Theta = \Delta\phi(t)$.

2.2 Signal Processing -Source Separation (ICA)

Independent component analysis (ICA) is a statistical method that performs the transformation of a multi-dimensional random vector observations into sources that are statistically as independent from each other as possible [10] and generally uses techniques involving higher order statistics [13]. The different implementation of ICA can be found in the literature [2, 6, 11] and we will be only focussing on the fastICA algorithm [10] in this application.

In essence, independent component analysis assumes that in a set of $m-$dimensional measured time series vector denoted as $x(t) = [x_1(t), x_2(t), ...x_m(t)]^T$ to be a linear combination of n-dimensional source vectors whose components are assumed to be statistically independent and given as $s(t) = [s_1(t), s_2(t), ...s_n(t)]^T$. Further, it assumes that the dimension of x and s are equal, for instance $m = n$ [10]. ICA is often represented as

$$x(t) = As(t), \tag{10}$$

where A is a full rank $m \times n$ mixing matrix [13]. Then, a separating or de-mixing matrix W must be estimated under certain assumptions and constraints [10] in order to extract each independent source signal from the observations such that

$$s(t) = Wx(t). \tag{11}$$

FastICA is based on a fixed point iteration scheme that attempts to separate the underlying sources from a given set of mixed measurements (observations) by finding their maximum of the non-Gaussianity, $w^T x$, as measured in equation 12. Here, the measure of non-Gaussian-ity, negentropy $J(y)$ is based on the information theoretic quantity of differential entropy which can be is given as $J(y) = H(y_{gauss} - H(y))$. Here $H(.)$ is the differential entropy and y_{gauss} is a Gaussian random variable with the same covariance matrix as output signal y. In FastICA, the approximation of the negentropy was referrerd as,

$$J(y) \approx \rho[EG(y) - EG(v)]^2, \tag{12}$$

where ρ is a positive constant, v is a Gaussian variable with zero mean and unit variance and $G(.)$ is any non-quadratic function as typically suggested in [10].

The basic form of the fastICA algorithm (one unit) can be denoted as follows:

Algorithm 1 FastICA

1: **procedure** FASTICA
2:     Data centering
3:     Whitening
4:     Initialize weight vector, w,
5: *loop*:
6:     $w^+ = E\{xg(w^T x)\} - E\{g'(w^T x)\}$,
7:     $w = \frac{w^+}{\|w^+\|}$,
8:     goto loop if not converged.

where g is the derivative of the non-quadratic function G, for instance;

$$G_1(u) = \frac{1}{a_1} log.cosh(a_1 u),$$
$$g_1(u) = tanh(a_1 u),$$
$$g_1'(u) = a(1 - tanh^2(a_1 u)). \tag{13}$$

Here, $1 \le a \le 2$ is a suitable constant, normally taken as $a = 1$. To estimate several independent components (IC), the basic form of one unit FastICA needs to be extended using several units with weight vectors $w_i, i = 1, 2...n$. The outputs $w_1^T x, ..., w_n^T$ need to be decorrelated to prevent vectors from converging to the same maxima after every iteration [12]. One method of achieving decorrelation is through Gram-Schmidt like decorrelation where estimation of IC is performed one by one. When p Independent Components or $p-$vectors $w_1, ..., w_p$ were estimated, one unit FastICA is performed for w_{p+1} and after each iteration, the projections of $w_{p+1}^T w_j w_j, j = 1, ..., p$ of the previously estimated p vectors are subtracted from w_{p+1} and renormalized. The entire process can be represented as

$$1. Let \quad w_{p+1} = w_{p+1} - \sum_{j=1}^{p} w_{p+1}^T w_j w_j,$$

$$2. Let \quad w_{p+1} = w_{p+1} / \sqrt{w_{p+1}^T w_{p+1}}. \tag{14}$$

Another approach to achieve decorrelation is through a symmetric decorrelation where no vectors are "priviliged" over others [12, 14]. It can be implemented via a classical method involving matrix square roots as follows [12]:
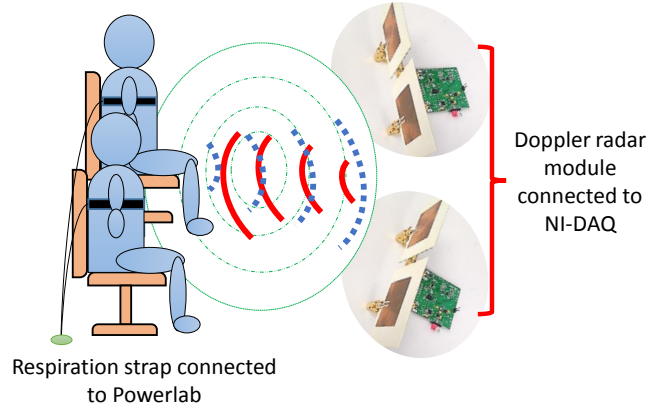
1. Let $W = (WW^T)^{-0.5} W$,

where W is the matrix of $w_1, ..., w_n$ of the vectors. The inverse square root of $(WW^T)^{-0.5}$ is computed from the eigenvalue decomposition WW^T [14]. A more simplistic alternative is given in the form of the following iterative algorithm [10],
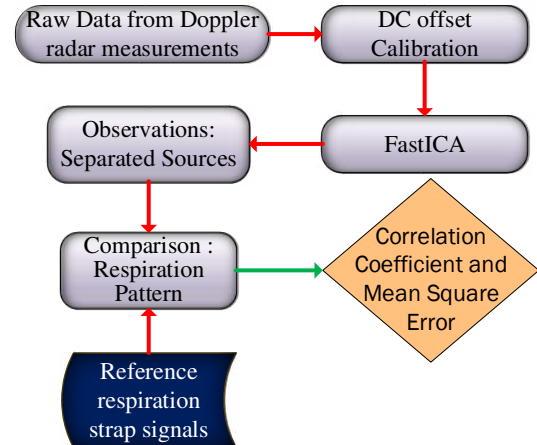
1. Let $W = W / \sqrt{\|WW^T\|}$

2. Let $W = 1.5W - 0.5WW^T W$

3. Repeat 2 until converges.

3 Experiment Protocol for Real Data Sensing

(a) Experimental Setup for the Data Acquisition of two subjects

(b) General Flow of the Source Separation process

Experiment	Person 1	Person 2
1 (2 Subjects)	Normal	Normal (faster pace)
2 (2 Subjects)	Normal + apnea	Normal
3 (1 Subject)	Normal + Arm swinging	Nil

(c) Experimental Protocol for Different modes of Breathing

Fig. 1 Experiment Setup, Signal Processing Flow and Experiment Protocol

The measurement of human respiration using the non-contact Doppler radar was approved by the Faculty of Science and Technology Ethics Sub-Committee HEAG (Faculty Human Ethics Advisory Groups), Deakin University and all the participants provided their writ-

ten informed consent to participate in these experiments.

In this experiment, two 2.4 GHz Doppler radar modules [8] were used to capture the respiration signals from two subjects (in each experiment) as shown in Figure 1(a). Each of the systems transmitted a continuous wave (CW) of 2.4 GHz and was attached to two patch antennae (transmitter and receiver) connected to a data acquisition module (DAQ: NI-USB6009). The received signals were then further processed in a MATLAB environment. In each experiment, the subjects were positioned 1 metre away from the antennae where the antennae were aligned to focus on the abdomen of the subjects. Respiration signals from the subjects were collected with normal clothing and in a seated position in the laboratory. An external respiration strap (MLT1132 Piezo Respiratory Belt Transducer) attached to Power-Lab (ADInstruments) was used as a reference signal to evaluate the performance results of the source separation technique on the measurements obtained from the Doppler radar.

Two sets of experiments were then carried out to evaluate the separation technique between two breathing signals captured from the Doppler radar measurements. In the first experiment, two subjects were breathing normally but at different rates while in the second experiment, one of the subjects was breathing normally while the other subject role played apnea by stopping the breathing for a certain duration multiple times. The last experimental trial was performed on one subject under the influence of motion artefacts (arm swing). The summary of the experiments are shown in Figure 1(c). The general flow of the source separation process is shown in Figure 1(b).

4 Results

4.1 Two Simulated Respiratory Sources

In order to commence with the basic idea of source separation, two sources mimicking respiration were considered in this simulation. As depicted in Figure 2, two respiration baseband signals (with a DC offset and Gaussian noise) at 0.20 Hz and 0.28 Hz respectively were simulated using equations 3 and 4. Then, the baseband signals (in-phase (I) and quadrature-phase (Q)) were randomly mixed (see equations 8 and 9) and re-calibrated to eliminate the DC offset. From the constellation plot, it was evident that DC offsets have been corrected. In this particular step, we have used the curve fitting technique [21] to fit the I and Q data to a circle as shown in Figure 2. Two different frequency spectra were clearly

observed from the spectrum plot denoting the respective baseband respiration frequencies that were simulated. The main aim of this simulation was to evaluate the source separation technique in separating the simulated Doppler radar combined baseband respiration signals into its relevant independent sources while preserving the frequency and the breathing pattern information.

In this simulation, fast fixed-point algorithm for independent component analysis (fastICA) was used. From the results shown in Figure 2, the mixed signals were successfully separated where the approximated spectral frequencies were 0.2014 Hz and 0.2808 Hz respectively. This was achieved while preserving similarity of the baseband signal pattern to the simulated respiration signals. From the simulation, it was observed that by using the in-phase signals from two baseband signals, the spectral frequency and the patterns of the baseband gave a better representation rather than using the quadrature-phase signals.

4.2 Experiment involving real subjects

Simulation results indicated promising results in separating the mixed signals from the respective I/Q channel into its respective independent component of baseband respiration signal. Thus, we have implemented the corresponding algorithm with the real respiration measurement data from the Doppler radar. For these particular experiments, two subjects were located in front of two Doppler radar transceivers while breathing according to the conditions listed in figure 1(c). In the first experiment, two subjects were asked to breathe normally at different rates while in the second experiment, one of the subjects was asked to hold their breath (role playing central apnea) while the other subject was continually breathing in a normal mode.

Figure 3(a) depicts a compilation of the results observed from experiment 1. The raw mixed I signals were pre-processed for DC offset calibration before the separation process. From one of the spectrum plots in the calibrated mixed I signals, there were two dominant breathing frequencies of 0.3052 Hz and 0.4425 Hz. The expected outcome of this experiment would be two respiration signals from two different subjects in terms of the respiration rates and patterns. For this purpose, we have use the fastICA algorithm to separate the mixed I signals into its independent components where the separation results were then compared to the independent measurements of the respiration strap. The results are shown in Table 1(a) in terms of the mean square error (MSE) and correlation coefficient (Corr). Under normal
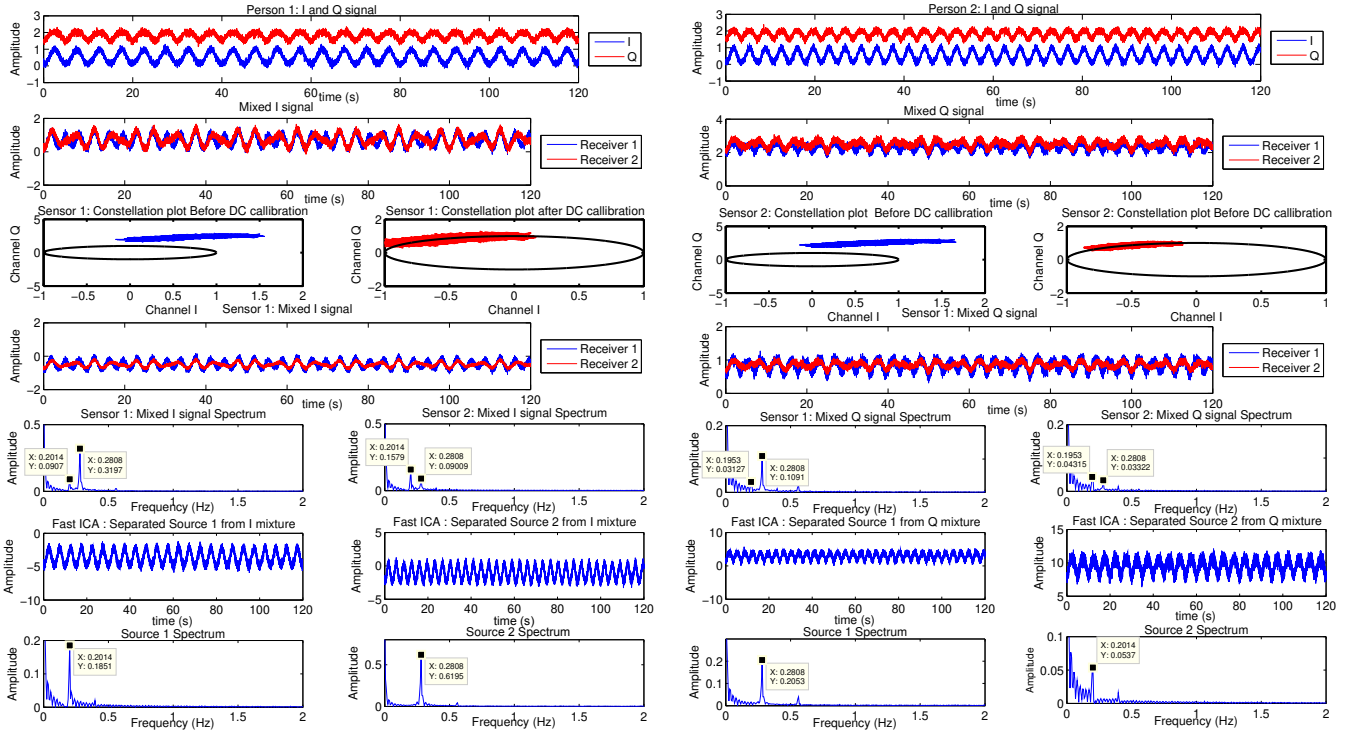
Fig. 2 Two simulated sources with Normal Breathing captured from Doppler radar modules. Figure (from top row to bottom row): Baseband signal of two respiration signals; Randomly mixed baseband signals; Constellation plot before and after DC offset calibration; Mixture of sources after DC calibration; Frequency spectrum of the mixture; Independent sources; Frequency spectrum of the independent sources

breathing conditions, the respiration rate can be estimated using fast fourier transform (FFT) [9, 17] and as shown in Figure 3(a), the breathing rates estimated from the independent respiration strap were similar to the breathing frequency of each independent source derived from fastICA (using the measurements acquired from the Doppler radar).

As for the second experiment, the results of the source separation are shown in Figure 3(b). In this particular experiment, one of the subjects was asked to hold his breath multiple times in two minutes of recording to mimic the condition of central sleep apnea [5]. This experiment was specifically designed to evaluate fastICA source separation capabilities in dealing with the mixed signals of normal breathing and abnormal breathing patterns. As shown in Figure 3(b), (see Figure 3(b): (e)), the results show the occurrence of multiple cessation of breathing in the patterns which corresponds to the central apnea type of breathing. The derived independent component for this is highly correlated with the independent measurement of the respiration strap. As for the second subject, a normal breathing pattern was observed (see Figure 3(b): (f)) as expected. From the spectral analysis (see Figure 3(b): (h)), the normal breathing source was successfully sep-

arated from the mixed sources where the peak of 0.3815 Hz was detected in both the reference respiration strap and the separated source. As for the spectral analysis shown in Figure 3(b)(g), the FFT based evaluation for abnormal respiration pattern is not a good measure to estimate the respiration frequency. A technique such as time-frequency analysis is needed to cater for such respiration dynamics [17]. The qualitative evaluation of this experiment is shown in Table 1(b).

5 Further Discussion

We have also performed the separation of sources using fastICA with different type of non-linearities, i.e g functions (refer to Table 2) where the performance of each function was shown in Table 1(a) and Table 1(b) by comparing each independent source with the reference respiration strap. Considering data from four different subjects in two different experiments, *tanh* as the g function performs better(in terms of MSE) in separating the sources from the Doppler radar based measurements compared to other common non-linear functions considered. A reasonable correlation with shorter processing time was observed as shown in Figure 4.
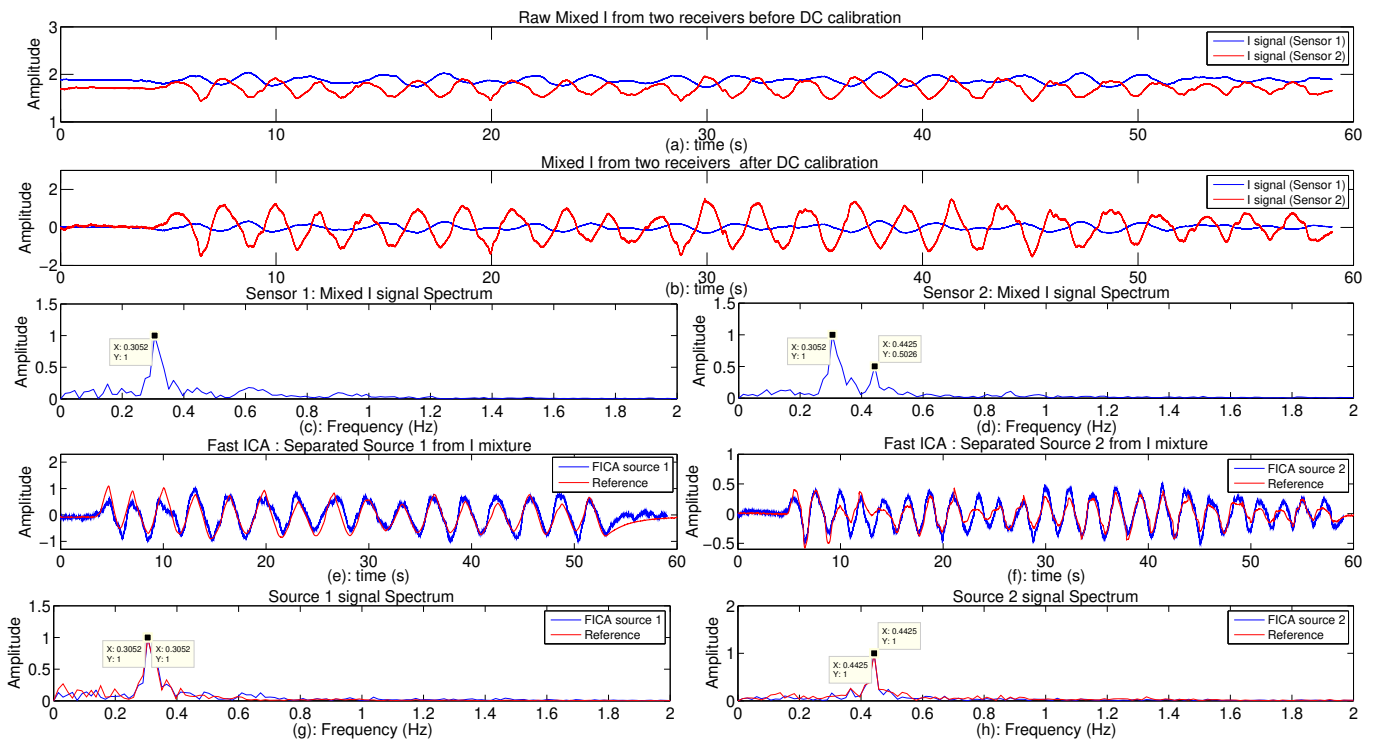
(a) **Normal Breathing**
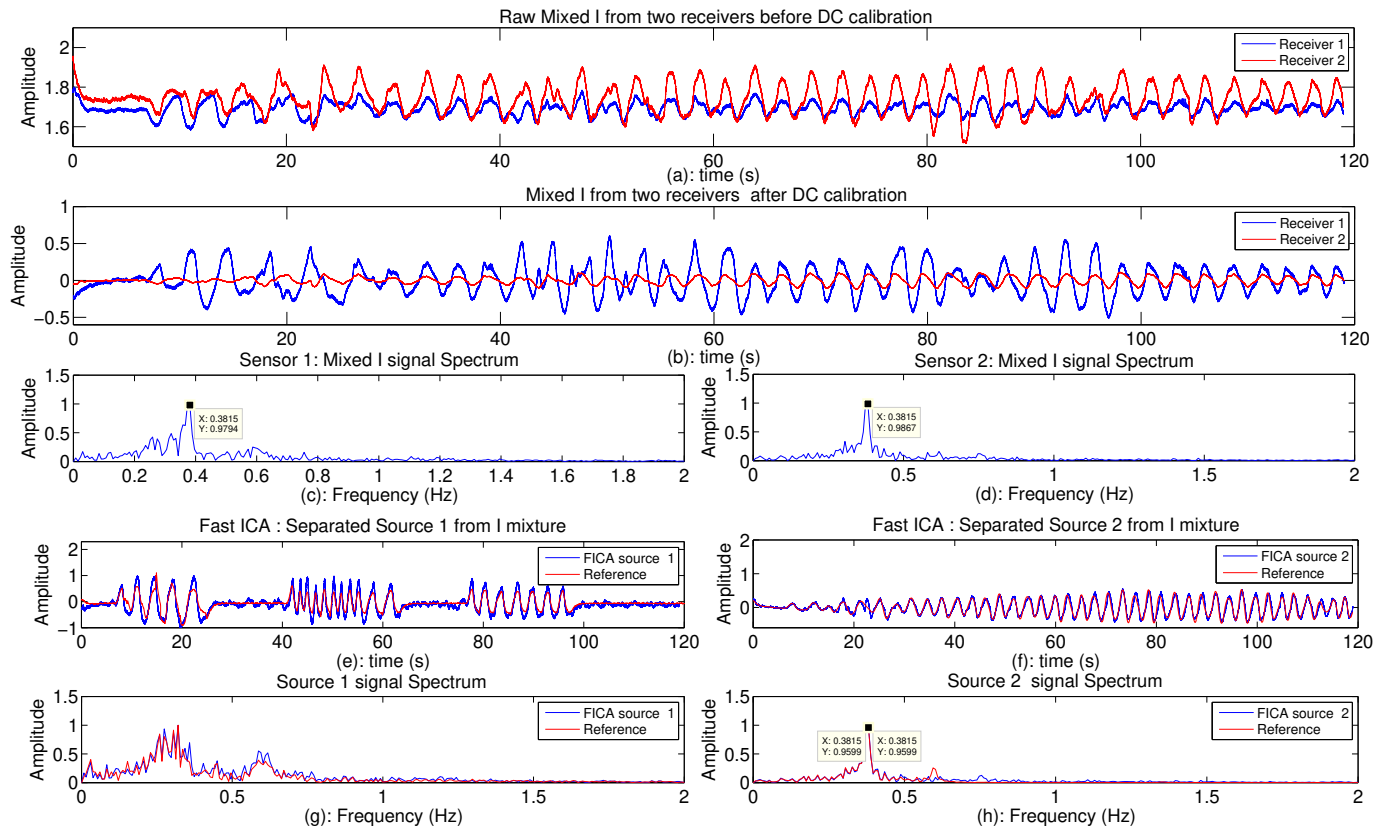
(b) **Normal Breathing with apnea Characteristic**

Fig. 3 Two source breathing signals captured from Doppler Radar modules (top to bottom) :(a) Raw data of mixed in-phase (I) signal; (b) DC offset calibrated mixed I signal; (c), (d) Spectrum of each mixed I channel signals; (e), (f) Separated breathing source for each subject; (g), (h) Spectrum of each independent breathing component

Table 1 Performance Evaluation on FastICA using different non-linearity g function with Reference Respiration Strap Signal Patterns

(a) Experiment 1

| g function | Source 1 | | Source 2 | | |
	MSE	Corr	MSE	Corr	Time (s)
tanh	**0.2055**	**0.8765**	**0.0474**	**0.8811**	**0.0536**
power	0.2098	0.8765	0.0838	0.8819	0.0575
gauss	0.2068	0.8764	0.0473	0.8809	1.3024
skew	0.2207	0.7959	0.0372	0.7737	1.2907

(b) Experiment 2

| g function | Source 1 | | Source 2 | | |
	MSE	Corr	MSE	Corr	Time (s)
tanh	**0.1670**	**0.9080**	**0.1280**	**0.9543**	**0.0766**
power	0.1717	0.9071	0.1281	0.9543	0.1183
gauss	0.1713	0.9072	0.1279	0.9543	0.0926
skew	0.1766	0.9057	0.1269	0.9520	1.7229

We have also evaluated the performance of various BSS algorithms [20] on all the datasets and the results are given in Table 3(a) & 3(b). The tested algorithms include EFICA [15], WASOBI [23], COMBI [24], MCOMBI [25], FCOMBI [7], BEFICA [15] and BARBI [22]. From the results, most of the BSS algorithms are capable of performing the separation with a low MSE and good correlation coefficient but fastICA with *tanh function* performs better; more suitable for real time applications particularly due to shorter processing time.
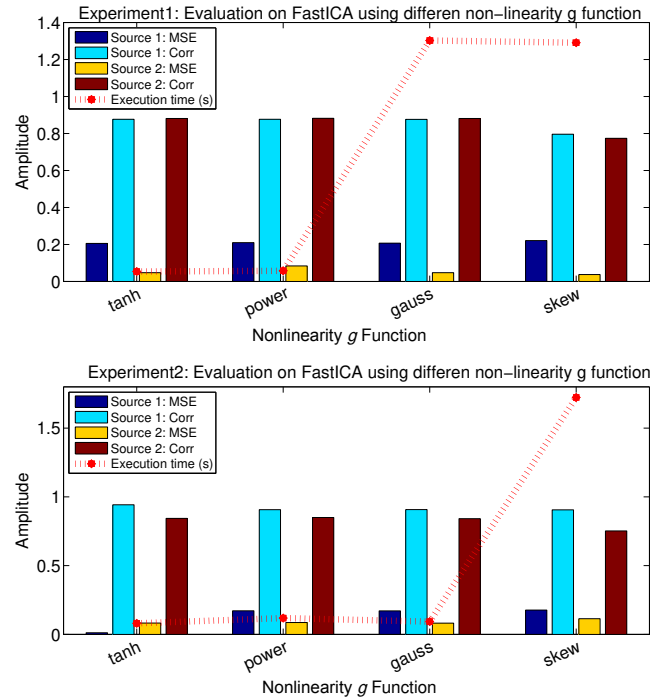
Table 2 Non-linearity of g function

Nonlinearity	g(u)
tanh	$g(u) = tanh(au)$
power	$g(u) = u^3$
gauss	$g(u) = u * \exp(-au^2/2)$
skew	$g(u) = u^2$

Fig. 4 Pictorial representation of the Performance Evaluation of FastICA using different non-linear functions with Reference to Respiration Strap Signal Patterns

5.1 Separation of Hand Motion

In addition to the decomposition of signals, we have also explored the use of fastICA in the removal of motion artefacts. In particular, we investigated separating the respiratory signal from a typical interfering signal, i.e a subject's right arm movement as a a motion artefact. The performance of the separation task is shown in the figure 5. The separated hand motion from the mixture of signals is clearly observed in Figure 5(d) as marked, while the filtered respiration signal pattern is shown in Figure 5(c).

Although the motion due to the swinging of the arm is separated from the mixture of the signals, the separated respiration signal is not entirely free from other noise inputs (for instance, possible artefacts due to the slight motion of the body during the swinging process) as shown in Figure 5(c). Therefore, even for the case of respiration detection involving a single subject, the

use of a multiple antenna configuration would significantly improve the coverage, detection and the characterisation capabilities of human motion in general. For instance, in characterising the capabilities of human motion, multiple antennas can be used to identify the motion from various bodies parts such as leg, arm or head in correspondence to the placement of the antenna. In particular sleep studies where periodic limb movements are of interest, the source separation can be used to analyse the artefacts.

Typically, DWT uses a dyadic grid [1] where the dyadic wavelet transform of signal $s(t)$ is given as:

$$DWT\ s(m,n) = 2^{-m/2} \int_{-\infty}^{\infty} s(t)\varphi * (\frac{t - 2^m n}{2^m})dt, \quad (15)$$

Table 3 Performance Evaluation on different BSS algorithms separated sources with Reference Respiration Strap Signal Patterns for Experiment 1

(a) Experiment 1

Algorithm	Source 1 MSE	Source 1 Corr	Source 2 MSE	Source 2 Corr	Time (s)
EFICA	0.2055	0.8765	0.0472	0.8832	0.2118
WASOBI	0.1566	0.7683	0.0437	0.8037	0.3643
COMBI	0.2053	0.8765	0.0472	0.8832	0.2097
MCOMBI	0.2053	0.8765	0.0472	0.8832	0.1700
FCOMBI	0.2053	0.8765	0.0472	0.8832	0.1629
BEFICA	0.1922	0.8751	0.0469	0.8837	0.2841
BARBI	0.2332	0.8434	0.0473	0.8745	0.1309

(b) Experiment 2

Algorithm	Source 1 MSE	Source 1 Corr	Source 2 MSE	Source 2 Corr	Time (s)
EFICA	0.1752	0.9063	0.1264	0.9514	0.1044
WASOBI	0.1797	0.9043	0.1253	0.9502	0.0456
COMBI	0.1752	0.9063	0.1264	0.9514	0.1015
MCOMBI	0.1752	0.9063	0.1264	0.9515	0.1228
FCOMBI	0.1753	0.9062	0.1265	0.9515	0.1763
BEFICA	0.1783	0.9050	0.1286	0.9535	0.1745
BARBI	0.1671	0.7314	0.1198	0.9539	0.0432
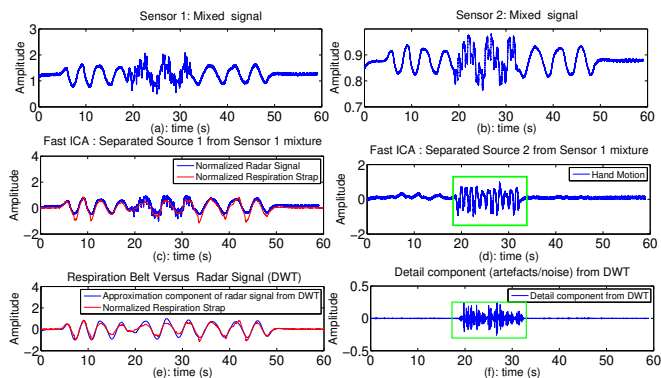
Fig. 5 A mixture of breathing signals with hand motion (swinging of the arm) from one subject. (a) & (b) are the mixtures of the signal from two antennas; (c) & (d) are the separated breathing source/hand motion signals (using FastICA) (e) & (f) are the filtered breathing source (DWT-Approximation component) and the filtered hand motion/noise signal source (DWT-Detailed component)

where m and n are scale and time shift parameters respectively, $*$ is the complex conjugate and $\varphi(t)$ is the given basis function (mother wavelet).

In general, the output of the low pass filter is known as wavelet approximation (scaling) coefficient cA_m and the output of the high pass filter is called wavelet detail coefficient cD_m [4,27]. The approximation and the detail coefficient at the mth level can be denoted as (16) and (17) respectively.

$$cA_m[n] = \sum_{-\infty}^{\infty} l_d[k]cA_{m-1}[2n-k], \tag{16}$$

$$cD_m[n] = \sum_{-\infty}^{\infty} h_d[k]cA_{m-1}[2n-k], \tag{17}$$

The taps of the high-pass filter h_d and the low pass filter l_d are derived from the scaling and wavelet function of a chosen mother wavelet family, i.e Daubechies, Haar or Coiflet.

As shown in Figure 5 (e), we used Discrete Wavelet Transform (DWT) to filter the artefacts/noise from the signal mixture where the reconstructed respiration signal (approximation component from DWT) is highly correlated and smoother than the results obtained from fastICA. Type of wavelet used in this experiment trial is Daubechies (Db10) with 10 levels of decomposition. The motion artefacts/noise can be obtained from the detail components as shown in Figure 5 (f). The DWT technique is particularly useful in filtering the artefacts/noises from the mixture of signals due to its nature. From our observations, this is not the case in separating multiple respiration sources due to multiple subjects.

As the main focus of this paper is the separation of respiration sources (multiple subjects) using fastICA, the exploration of using DWT for the removal of artefacts is not discussed here. Indeed the DWT technique can be useful and yield a better result compared to blind source separation technique as demonstrated in [26] and more importantly, it can be implemented with only a single antenna configuration. Nevertheless, using DWT solely will not improve the respiration detection coverage; specially when more than one source of respiration exists which is the main focus of this paper.

6 Conclusion

In this paper, we investigated respiration detection using Doppler radar involving multiple subjects incorporating the use of the multiple Doppler radar systems. The need to measure multiple sources in respiratory monitoring is essential specially for long-term home-based monitoring applications(i.e. sleep apnea, sleep studies) where typically more than one person is in a bed. For this purpose, we have demonstrated the use of the fastICA algorithm in separating the mixed Doppler radar measurements of two people under two different scenarios involving either normal breathing only or ab-

normal breathing (mixture of normal breathing and apnea) as discussed in the experiment protocol.

From the source separation results, it was shown that we are able to estimate the breathing rate as well as to identify corresponding respiratory patterns associated with normal breathing and apnea symptoms accurately. Further, we have also investigated the separation of motion artefacts from the mixed respiration signals using fastICA where the motion due to the swinging of the subject's arm can be identified from the Doppler shifted data. In conclusion, we used a multiple antenna configuration to demonstrate the possibility of decomposing a Doppler radar based respiratory patterns into separate sources using fastICA even when the sources are potentially interfered by motion artefacts.

Future work would be extended to involve respiration measurements under the influence of motion artefacts. These artefacts, i.e. movement of the body and the jerking of the arm, will be studied thoroughly to be incorporated as the prior knowledge to the source separation algorithm in order to obtain the desired respiratory signatures as well as to isolate the artefact signature. These artefacts signature could be of use in certain sleep studies.

References

1. Addison, P.S.: Wavelet transforms and the ecg: a review. Physiological measurement 26(5), R155 (2005)
2. Bell, A.J., Sejnowski, T.J.: An information-maximization approach to blind separation and blind deconvolution. Neural computation 7(6), 1129–1159 (1995)
3. Boric-Lubecke, O., Lubecke, V., Host-Madsen, A., Samardzija, D., Cheung, K.: Doppler radar sensing of multiple subjects in single and multiple antenna systems. In: Telecommunications in Modern Satellite, Cable and Broadcasting Services, 2005. 7th International Conference on. vol. 1, pp. 7–11 vol. 1 (Sept 2005)
4. Bruce, L.M., Koger, C.H., Li, J.: Dimensionality reduction of hyperspectral data using discrete wavelet transform feature extraction. Geoscience and Remote Sensing, IEEE Transactions on 40(10), 2331–2338 (2002)
5. Chokroverty, S.: Sleep Disorders Medicine. Elsevier Inc (2009)
6. Comon, P.: Independent component analysis, a new concept? Signal processing 36(3), 287–314 (1994)
7. Gómez-Herrero, G., Koldovskỳ, Z., Tichavskỳ, P., Egiazarian, K.: A fast algorithm for blind separation of non-gaussian and time-correlated signals. In: Proccedings of the 15th European Signal Processing Conference. EUSIPCO. pp. 2007–07. Citeseer (2007)
8. Gu, C.: 2.4 ghz multifunctional software-defined radar sensor system. `http://www.webpages.ttu.edu/chgu/resource.html`
9. Gu, C., Long, J., Huangfu, J., Qiao, S., Cui, W., Ma, W., Ran, L.: An instruments-built doppler radar for sensing vital signs. In: Antennas, Propagation and EM Theory, 2008. ISAPE 2008. 8th International Symposium on. pp. 1398–1401 (2008)
10. Hyvärinen, A.: Fast and robust fixed-point algorithms for independent component analysis. Neural Networks, IEEE Transactions on 10(3), 626–634 (1999)
11. Hyvärinen, A., Karhunen, J., Oja, E.: Independent component analysis, vol. 46. John Wiley & Sons (2004)
12. Hyvärinen, A., Oja, E.: Independent component analysis: algorithms and applications. Neural networks 13(4), 411–430 (2000)
13. James, C.J., Gibson, O.J.: Temporally constrained ica: an application to artifact rejection in electromagnetic brain signal analysis. Biomedical Engineering, IEEE Transactions on 50(9), 1108–1116 (2003)
14. Karhunen, J., Oja, E., Wang, L., Vigario, R., Joutsensalo, J.: A class of neural networks for independent component analysis. Neural Networks, IEEE Transactions on 8(3), 486–504 (1997)
15. Koldovsky, Z., Tichavsky, P., Oja, E.: Efficient variant of algorithm fastica for independent component analysis attaining the cram&# 201; r-rao lower bound. Neural Networks, IEEE Transactions on 17(5), 1265–1277 (2006)
16. Lee, Y.S., Pathirana, P., Robin.J., E., Steinfort, C.: Noncontact detection and analysis of respiratory function using microwave doppler radar. Journal of Sensors (2015)
17. Lee, Y.S., Pathirana, P., Steinfort, C., Caelli, T.: Monitoring and analysis of respiratory patterns using microwave doppler radar. Translational Engineering in Health and Medicine, IEEE Journal of 2, 1–12 (2014)
18. Obeid, D., Sadek, S., Zaharia, G., El Zein, G.: Touchless heartbeat detection and cardiopulmonary modeling. In: Applied Sciences in Biomedical and Communication Technologies, 2009. ISABEL 2009. 2nd International Symposium on. pp. 1 –5 (nov 2009)
19. Oum, J.H., Kim, D.W., Hong, S.: Two frequency radar sensor for non-contact vital signal monitor. In: Microwave Symposium Digest, 2008 IEEE MTT-S International. pp. 919 –922 (june 2008)
20. Petkov, J., Koldovskỳ, Z.: Bssgui–a package for interactive control of blind source separation algorithms in matlab. In: Cross-Modal Analysis of Speech, Gestures, Gaze and Facial Expressions, pp. 386–398. Springer (2009)
21. Taubin, G.: Estimation of planar curves, surfaces, and nonplanar space curves defined by implicit equations with applications to edge and range image segmentation. IEEE Transactions on Pattern Analysis and Machine Intelligence 13(11), 1115–1138 (1991)
22. Tichavsky, P., Yeredor, A., Koldovsky, Z.: A fast asymptotically efficient algorithm for blind separation of a linear mixture of block-wise stationary autoregressive processes. In: Acoustics, Speech and Signal Processing, 2009. ICASSP 2009. IEEE International Conference on. pp. 3133–3136 (April 2009)
23. Tichavskỳ, P., Doron, E., Yeredor, A., Nielsen, J.: A computationally affordable implementation of an asymptotically optimal bss algorithm for ar sources. Proc. EUSIPCO-2006 pp. 4–8 (2006)
24. Tichavskỳ, P., Koldovskỳ, Z., Doron, E., Yeredor, A., Gómez-Herrero, G.: Blind signal separation by combining two ica algorithms: Hos-based efica and time structure-based wasobi. In: Eur. Signal Process. Conf.(EUSIPCO), Florence (2006)

25. Tichavsky, P., Koldovsky, Z., Yeredor, A., Gómez-Herrero, G., Doron, E.: A hybrid technique for blind separation of non-gaussian and time-correlated sources using a multicomponent approach. Neural Networks, IEEE Transactions on 19(3), 421–430 (2008)
26. Vergara, A., Petrochilos, N., Boric-Lubecke, O., Host-Madsen, A., Lubecke, V.: Blind source separation of human body motion using direct conversion doppler radar. In: Microwave Symposium Digest, 2008 IEEE MTT-S International. pp. 1321–1324. IEEE (2008)
27. Villasenor, J.D., Belzer, B., Liao, J.: Wavelet filter evaluation for image compression. Image Processing, IEEE Transactions on 4(8), 1053–1060 (1995)
28. Xu, W., Gu, C., Li, C., Sarrafzadeh, M.: Robust doppler radar demodulation via compressed sensing. Electronics Letters 48(22), 1428–1430 (2012), `http://link.aip.org/link/?ELL/48/1428/1`
29. Yan, Y., Li, C., Yu, X., Weiss, M., Lin, J.: Verification of a non-contact vital sign monitoring system using an infant simulator. In: Engineering in Medicine and Biology Society, 2009. EMBC 2009. Annual International Conference of the IEEE. pp. 4836 –4839 (sept 2009)
30. Yuan, G., Drost, N.A., McIvor, R.A.: Respiratory rate and breathing pattern. McMaster University Medical Journal 10, 23–28 (2013)

Author/s:
Lee, YS;Pathirana, PN;Evans, RJ;Steinfort, CL

Title:
Separation of Doppler radar-based respiratory signatures

Date:
2016-08-01

Citation:
Lee, Y. S., Pathirana, P. N., Evans, R. J. & Steinfort, C. L. (2016). Separation of Doppler radar-based respiratory signatures. MEDICAL & BIOLOGICAL ENGINEERING & COMPUTING, 54 (8), pp.1169-1179. https://doi.org/10.1007/s11517-015-1379-3.

Persistent Link:
http://hdl.handle.net/11343/282721